

Contribution of Rock Glacier Discharge to Late-Summer and Fall Streamflow in the Uinta Mountains, Utah, USA

Jeffrey S. Munroe¹, Alexander L. Handwerker^{2,3}

¹ ~~Geology~~ Department of Earth & Climate Sciences, Middlebury College, Middlebury, 05753, USA

² Joint Institute for Regional Earth System Science and Engineering, University of California, Los Angeles, 90095, USA

³ Jet Propulsion Laboratory, California Institute of Technology, Pasadena, 91109, USA

Correspondence to: Jeffrey S. Munroe (jmunroe@middlebury.edu)

Abstract. Water draining from rock glaciers in the Uinta Mountains of Utah (USA) was analyzed and compared with samples of ~~ground water~~ groundwater and water from the master stream in a representative 5000-ha drainage. Rock glacier water resembles snowmelt in the early summer, but ~~transitions evolves~~ to higher values of *d-excess* and greatly elevated Ca and Mg content as the melt season progresses. This pattern is consistent with models describing a transition from snowmelt, to melting of seasonal ice, to melting of perennial ice in the rock glacier interior in late summer and fall. Water derived from this internal ice appears to have been the source of ~25% of the streamflow in this study area during September of 2021. This result emphasizes the significant role that rock glaciers can play in the hydrology of high-elevation watersheds, particularly in summers following a winter with below average snowpack.

Keywords: Rock glacier; hydrology; permafrost; stable isotopes; climate change

1 Introduction

Contemporary climate change is responsible for an array of dramatic effects in high mountain environments (Adler et al., 2019; Chakraborty, 2021). Average temperatures of air (Bonfils et al., 2008; Minder et al., 2018) and permafrost (Biskaborn et al., 2019) are rising, glaciers are retreating (Sakai and Fujita, 2017; Sommer et al., 2020), the ranges of plants (Alexander et al., 2018; Albrich et al., 2020) and animals (Millar and Westfall, 2010; Rödder et al., 2021) are shifting, and ecosystem services (Egan and Price, 2017; Palomo, 2017) and the societies that depend on them (McDowell et al., 2019; Xenarios et al., 2019) are in a phase of readjustment. Documenting and understanding these changes is of crucial importance in mitigating natural hazards (Stoffel and Corona, 2018; Thaler et al., 2018), anticipating future scarcity of water resources (Beniston et al., 2018; Rowan et al., 2018), designing appropriate conservation strategies (Catalan et al., 2017), and planning for a future in which mountain environments look and function differently than they have for the past century (Huss et al., 2017).

34 A component of mountain landscapes with strong potential to document past and present environmental
35 changes, and a notable vulnerability to climatic perturbations, are features known as rock glaciers. Typically present
36 in cold environments that are too dry for the formation of ice glaciers, rock glaciers are mixtures of rock debris and
37 perennial ice that move downslope through a combination of creep and basal shear (Wahrhaftig and Cox, 1959;
38 Giardino et al., 1987; Giardino and Vitek, 1988). Given their genesis, their composition, and their behavior, rock
39 glaciers exist at the intersection of climate, the cryosphere, and hydrology.

40 Traditionally, rock glacier research focused on the distribution and paleoclimatic significance of these
41 features (Konrad et al., 1999; Johnson et al., 2021). Modern updates to these investigations are applying high
42 precision GPS (Buchli et al., 2018), photogrammetry (Kenner et al., 2018), surface-exposure dating (Lehmann et al.,
43 2022), and remote sensing to monitor rock glacier movement (Strozzi et al., 2020), offering an unprecedented
44 understanding of the relationship between rock glacier behavior and climate change. Studies have also sought to
45 explore the role of rock glaciers as refugia for cold-adapted organisms in the face of warming temperatures (Millar
46 et al., 2015; Brighenti et al., 2021).

47 An additional ~~line of inquiry~~ topic with critical importance in regions characterized by water scarcity is the
48 contribution of rock glaciers to high mountain hydrology (Rangecroft et al., 2015; Jones et al., 2019). The
49 interconnected pore space within the typically coarse debris comprising a rock glacier allows these features to serve
50 as aquifers, storing and releasing water over a variety of timescales (Geiger et al., 2014; Harrington et al., 2018;
51 Wagner et al., 2020; Halla et al., 2021). Moreover, perennial ice within the interior of an active rock glacier is a
52 reservoir of longer-term storage that is nonetheless vulnerable to being lost from the system through melting in
53 excess of new ice formation. Studies have investigated the ice content of rock glaciers using geophysical methods
54 ~~like such as~~ ground penetrating radar and invasive approaches like drilling (Krainer and Mostler, 2002; Krainer et
55 al., 2015; Petersen et al., 2020; Wagner et al., 2021). Extrapolation from these investigations, and incorporation of
56 empirical transfer functions, has supported estimates of rock glacier water storage for some areas (Azócar and
57 Brenning, 2010; Rangecroft et al., 2015; Janke et al., 2017; Jones et al., 2018). Nonetheless, uncertainty remains
58 about how much ice is stored within rock glaciers, the vulnerability of this ice to climate warming, and how much
59 ice may already be melting and contributing to base flow, particularly in late summer after the melting of seasonal
60 snow has ceased.

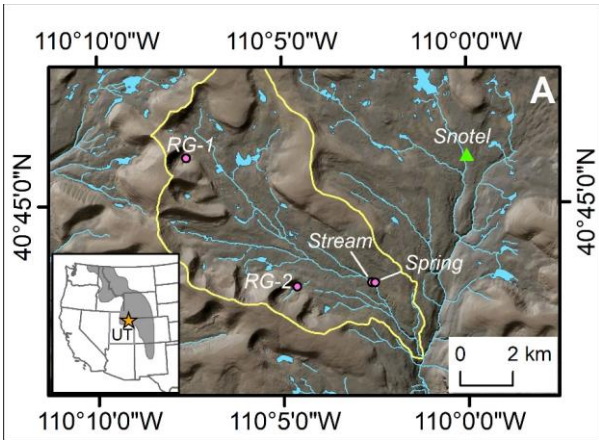
61 Here we investigate the water draining from representative rock glaciers in the Uinta Mountains in
62 northeastern Utah, a mountain range in which rock glaciers have been inventoried (Munroe, 2018) and monitored
63 (Brencher et al., 2021) in previous work. Automated samplers were used to collect time series of water discharging
64 from two rock glaciers, a non-rock glacier spring, and along the master stream. All samples were analyzed for
65 cation chemistry and stable isotopes to test two related hypotheses: 1) that the rock glacier springs would exhibit
66 properties distinct from the other water sources and consistent with the melting of internal ice in late summer; and 2)
67 that late summer streamflow along the master stream would contain a non-trivial amount of rock glacier-sourced
68 water.

69

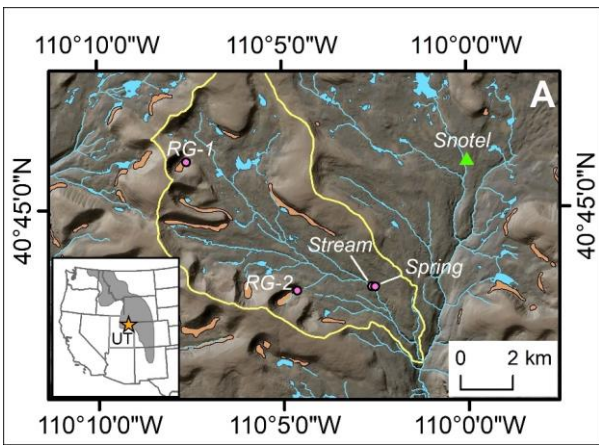
70 **2 Study Area**

71 The study area for this project is in the upper West Fork Whiterocks River watershed in the southeastern sector of
72 the Uinta Mountains (Figure 1). The watershed has an area of ~5000 ha above the lowest sampling site, and
73 elevations range from 2960 to over 3700 m. The Uinta Mountains (hereafter, the “Uintas”) are a substantial
74 component of the Rocky Mountain system located in northeastern Utah in the western United States. The Uintas are
75 the highest mountains in this region, reaching elevations in excess of 4 km. ~~Geologically, the~~ bedrock of the
76 Uintas is a thick sequence of Precambrian siliciclastic rocks that was uplifted during the Laramide orogeny
77 beginning in the early Paleogene (Sears et al., 1982; Hansen, 1986; Dehler et al., 2007). Pleistocene valley glaciers
78 eroded deep cirques and glacial canyons, and deposited massive lateral and end moraine systems (Atwood, 1909;
79 Munroe and Laabs, 2009). No ~~ice~~ glaciers remain in these ~~mountains~~ Uintas today, however the climate at higher
80 elevations, where mean annual temperatures are <0 °C (Munroe, 2006), supports patterned ground, talus, and
81 abundant rock glaciers. Previous work using optical imagery (Munroe, 2018) and satellite-based radar
82 interferometry (Brencher et al., 2021) identified more than 200 active rock glaciers in the Uintas, and many more
83 ~~rock glaciers~~ that are no longer moving. Eight rock glaciers totaling 170 ha are mapped within the West Fork
84 Whiterocks drainage (Figure 1).

85



86



87

88 **Figure 1:** Location Map of the study area. Inset shows location of the Uinta Mountains (orange star) within the state
 89 of Utah (UT). Gray shaded polygon represents the Rocky Mountains. Map presents the upper Whiterocks River
 90 watershed (yellow boundary), mapped rock glaciers (orange), the locations of the RG-1, RG-2, Stream, and Spring
 91 water samplers (pink circles), and the Chepeta SNOTEL site (green triangle).

92

93

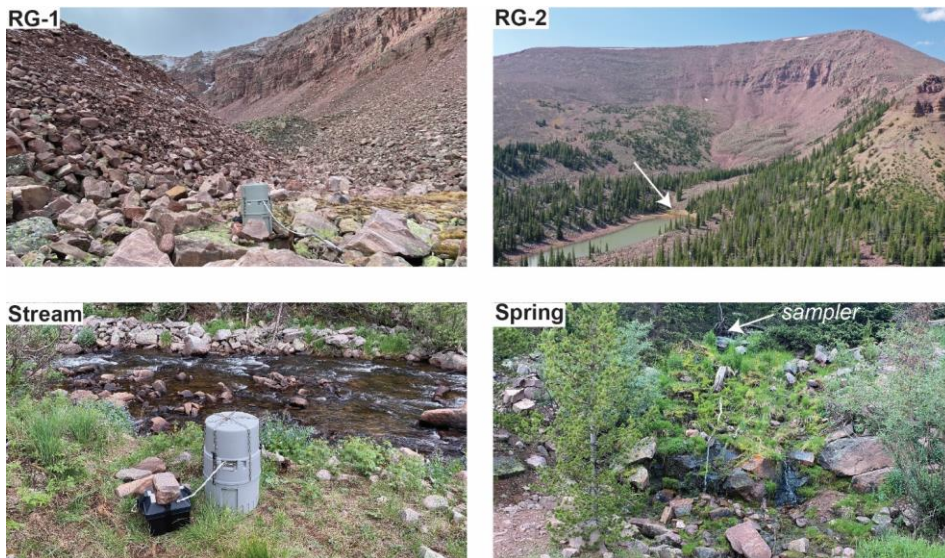
94

95 3 Methods

96 This project centered on the collection of time series of water samples using automated samplers outfitted with a
 97 carousel of 24 bottles. The samples were deployed with a solar powered battery system, allowing them to run

98 throughout the summer ~~with no maintenance~~. To reduce the possibility of isotopic fractionation related to
99 evaporation, sample bottles were modified following published methodology (von Freyberg et al., 2020). In each
100 location, the samplers were deployed in a position higher than their ~~water~~-intake to facilitate free draining of the
101 intake hose between samples. The weighted strainer on the end of the water intake line was wrapped in 100- μ m
102 nylon mesh to prevent coarse material from clogging the ~~sampler~~-pump. Each sampler was programmed to collect a
103 45-mL sample twice each day, at midnight and noon. For three days these samples (six samples total) were
104 composited in a single bottle, thus the 24 bottles in each sampler represented a maximum deployment duration of 72
105 days.

106 Two samplers were deployed at springs discharging from the base of rock glaciers that were the focus of
107 previous investigations (Munroe, 2018). These features, “RG-1” and “RG-2”, are typical of cirque floor, tongue-
108 shaped rock glaciers in the Uinta Mountains (Figures 1 and 2).



109
110 **Figure 2:** Pictures of water samplers at RG-1, RG-2, the Stream, and the Spring sites.

111
112 Each is approximately 600 m long, 100 m wide, and has steep frontal and side slopes standing up to 20 m tall. Fresh
113 exposures on these slopes reveal that the rock glaciers consist of several meters of coarse, openwork boulders
114 overlying a diamicton with a sand matrix. Internal ice is not exposed in either rock glacier, however data loggers
115 reveal that the springs maintain a temperature of 0 °C throughout the summer, and rock glacier surface temperatures
116 equilibrate at -5 °C or colder beneath winter snow cover (Munroe, 2018). Satellite InSAR (interferometric synthetic
117 aperture radar) analysis indicates that these features move slowly during the winter and accelerate during the

118 summer to velocities of ~10 cm/yr (Brencher et al., 2021). Collectively these observations suggest the presence of
119 ice within the rock glacier interior. The spring sampled at RG-1 has a typical summer discharge of 15 L/min. The
120 discharge at RG-2 was not measured directly, but a water-level logger records diurnal fluctuations of 0.2 (early
121 summer) to 0.02 m (late summer) of the lake into which the spring flows. Given the surface area of the lake (12,000
122 m²), these daily variations suggest a discharge on the order of 10² to 10³ L/min. In both cases these estimates are
123 approximations because much water likely drains belowground through the frost-shattered bedrock and glacial till
124 that mantles the surrounding landscape.

125 Two ~~other additional~~ water samplers were deployed at non-rock glacier locations. The “Spring” sampler
126 collected groundwater discharging from a typical spring unrelated to a rock glacier, and the “Stream” water sampler
127 was positioned slightly upstream along the main channel of the West Fork Whiterocks River, the master stream in
128 this drainage (Figure 1). These samplers were configured and programmed in an identical manner to those deployed
129 at the rock glacier springs.

130 To constrain the properties of precipitation in the study area, grab samples of snow were collected on the
131 surfaces of RG-1 and RG-2 when the water samplers were deployed. Water draining from a melting snowbank on
132 RG-2 was also collected. Rain was collected during the deployment period at the RG-2 and the Spring locations
133 using samplers ~~of a designed intended~~ to eliminate evaporation-related fractionation of isotope values (Gröning et
134 al., 2012). Given the sampler design, the rain samples are a composite of all precipitation accumulating during each
135 deployment period.

136 All samplers were installed at the beginning of July, 2021 (Table 1), which was the earliest date at which
137 the study area was accessible due to deep winter snow cover. At the Stream, Spring, and RG-2 samplers a
138 subsample was taken from the first bottle about a week later, with the remainder left inside the sampler. It was not
139 possible to revisit the more distant RG-1 sampler at this time. This procedure provided a check on the potential role
140 of evaporation fractionating the water samples as they waited inside the sampler. All bottles were emptied at the
141 beginning of September, and the samplers were relaunched to run until mid-October, when they were emptied again
142 and deactivated for the winter. The two precipitation samplers were emptied when the water samplers were
143 serviced. All samples for stable isotope analysis were filtered in the field to 0.2 µm and stored in 7-ml glass vials
144 with Teflon-lined caps. Samples for ICP-MS analysis were stored in 15-ml centrifuge tubes. These samples were
145 vacuum filtered with Whatman Number 1 paper in the lab and acidified to pH 2 with trace-element grade HNO₃. In
146 a preliminary phase of this project, daily samples were also collected at ~~the RG-2 spring~~ in the fall of 2020.

Sampler	Latitude	Longitude	Elevation (m)	Deployed	Emptied	Emptied	Duration (Days)
RG-1	40.766906	-110.127608	3408	7/2/2021	9/5/2021	10/7/2021	97
RG-2	40.721883	-110.076875	3197	7/1/2021	9/2/2021	10/6/2021	97
Spring	40.723016	-110.042131	2977	7/3/2021	9/2/2021	10/6/2021	95
Stream	40.722979	-110.043123	2965	7/3/2021	9/6/2021	10/6/2021	95

147

148 Stable isotope measurements were made with a Los Gatos 45-EP Triple Liquid Water Isotope Analyzer at
 149 Middlebury College. Samples were run against a bracketing set of 5 standards and calibrated with a cubic spline
 150 function. Each sample was analyzed 10 times, with the first 2 injections discarded to minimize cross-over.
 151 Standards were run as unknowns after every five samples as an internal check on the results. [Accuracy of the](#)
 152 [instrument is 0.4‰ for δD and 0.1‰ for δ¹⁸O. The standard deviation of repeat injections of the samples in this](#)
 153 [study was 0.17‰ for δD and 0.04‰ for δ¹⁸O.](#) Results were compared with the Global Meteoric Water Line-GMWL
 154 (Craig, 1961) as well as a Local Meteoric Water Line (LMWL) estimated from OIPC, the Online Isotopes in
 155 Precipitation Calculator (Bowen and Wilkinson, 2002; Bowen and Revenaugh, 2003). Values of *d-excess* were
 156 calculated as $d\text{-excess} = \delta D - (8 * \delta^{18}O)$ (Dansgaard, 1964).

157 Hydrochemical characterizations were made with a Thermo iCap ICP-MS at Middlebury College. Samples
 158 were run against a set of standards derived from NIST Standard Reference Material 1643f “Trace Elements in
 159 Water”. An in-house standard was used to determine the abundance of Si and Ti, which are not present in 1643f.
 160 The NIST standard and the in-house standards were run after every 10 unknowns and a linear correction was applied
 161 to compensate for instrument drift. Interpretation focused on elements that consistently exhibited concentrations >1
 162 ppb.

163

164 **4 Results**

165 ~~A total of 141 water samples were analyzed, consisting of 134 samples from the four time-series (including~~
 166 ~~the 3 duplicates), 4 samples of rain, 2 samples of snow, and 1 sample of snow melt. The time-series are essentially~~
 167 complete with no gaps between early July and mid-October. The lone interruption is one bottle from the Stream
 168 sampler, representing 18-20 July, that was empty, apparently because the ~~water river level in the river~~ briefly
 169 dropped below ~~the position of~~ the intake hose.

170 Overall values of δD in the time-series range from -118.94 to -83.71‰. Values of δ¹⁸O range from -16.36
 171 to -12.24‰, and δ¹⁷O from -9.13 to -6.39‰ (Table 2). The mean of δD is lowest in the Spring samples (-113.44‰)
 172 and highest at RG-1 (-91.24‰). The same pattern holds for mean values of δ¹⁸O and δ¹⁷O (Table 2). Values of *d-*
 173 *excess* are highest at the RG sites, and lowest (-10‰) in the Stream (Table 2). Values of δD and δ¹⁸O for the

174 subsamples from the first bottle in the Stream, Spring, and RG-2 samplers are quite similar to the remainder that was
175 left ~~inside in~~ the collector ~~during through~~ the summer (Figure 3).

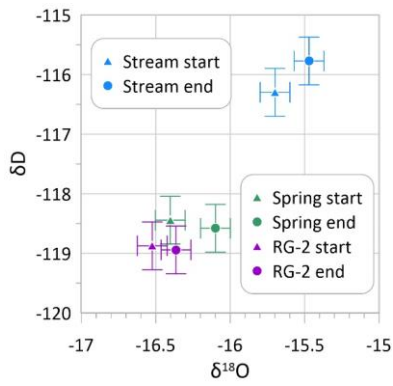


Figure 3: Comparison of isotope values measured for samples from RG-2, the Stream, and the Spring samplers. Subsamples were removed from the first sample in early July and the remainder of the water was left inside the collector until early September. Analysis of the sample pairs confirms that potential evaporation-related fractionation was minimal.

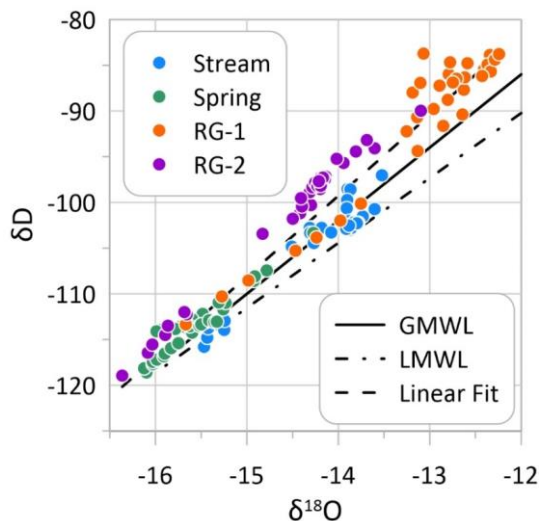
186

Table 2: Isotope Values for Water Samples				
	$\delta^2\text{H}$ (‰)	$\delta^{18}\text{O}$ (‰)	$\delta^{17}\text{O}$ (‰)	d-Excess (‰)
Stream (n=31)				
Mean	-103.86	-14.17	-7.38	9.52
Median	-102.55	-13.90	-7.40	9.02
Standard Deviation	4.92	0.57	0.31	1.52
Minimum	-115.77	-15.47	-8.06	7.97
Maximum	-97.05	-13.52	-6.78	12.62
Spring (n=33)				
Mean	-113.44	-15.57	-8.80	11.16
Median	-113.59	-15.60	-8.84	10.79
Standard Deviation	3.25	0.42	0.20	1.03
Minimum	-118.58	-16.12	-9.13	9.57
Maximum	-103.35	-14.28	-8.30	13.80
RG-1 (n=33)				
Mean	-91.24	-13.13	-6.94	13.83
Median	-87.22	-12.80	-6.62	13.87
Standard Deviation	8.52	0.88	0.60	2.59
Minimum	-113.35	-15.67	-8.48	9.80
Maximum	-83.71	-12.24	-6.39	20.82
RG-2 (n=34)				
Mean	-101.32	-14.53	-7.52	14.93
Median	-98.27	-14.24	-7.19	15.50
Standard Deviation	7.46	0.79	0.58	1.32
Minimum	-118.94	-16.36	-8.76	11.97
Maximum	-89.99	-13.10	-6.92	16.91

187

188 Values of δD and $\delta^{18}\text{O}$ are linearly and significantly ($p < 0.001$) related with a slope of 8.8 and a Y-intercept of
189 24.4‰ (Figure 4). Lower values of $\delta^{18}\text{O}$ plot closer to the GMWL; higher values of $\delta^{18}\text{O}$ plot increasingly above
190 the GMWL. Plotting the data from the individual samplers separately, with color coding by month, reveals
191 additional details (Figure 5). Values for the Stream and Spring samplers plot along the GMWL through the summer.
192 For the Stream, the lowest values are from July with higher values in late summer and fall. For the Spring, the
193 lowest values are again July, with the highest values in August; September and October values fall in between
194 (Figure 5). ~~On the other hand,~~ For the two rock glaciers, July values are ~~again lower~~ and closer to the GMWL, but
195 values from late summer and the fall plot notably above the GMWL with *d-excess* up to 20%. At RG-2, a similar

196 pattern was noted in daily samples collected during September, 2020 (Figure 5). Figures 4 and 5 also illustrate that
197 isotope values are significantly more depleted at RG-2 compared with RG-1.



198
199 **Figure 4:** Dual isotope plot of $\delta^{18}\text{O}$ and δD for the samples collected at RG-1, RG-2, the Stream, and the Spring.
200 The Global Meteoric Water Line (GMWL), a local meteoric water line (LMWL) determined from the Online
201 Isotopes in Precipitation Calculator (Bowen and Wilkinson, 2002; Bowen and Revenaugh, 2003), and a linear fit to
202 the data are presented for reference.

203
204 Plotting the data from the different samplers as time-series reveals patterns in the evolution of isotope
205 values during the sampling period (Figure 6). Given the strong correspondence between values of δD and $\delta^{18}\text{O}$,
206 only $\delta^{18}\text{O}$ is presented for clarity. Values are low at the start of the sampling period (early July), and generally rise
207 in all records through the summer and early fall (Figure 6A). The Spring and RG-2 both start below -16‰; the
208 Stream and RG-1 start slightly higher, near -15.5‰. All of the records exhibit transient spikes to less negative
209 values that occur quickly and taper gradually back to background levels (Figure 6A). These spikes align with pulses
210 of precipitation recorded at the Chepeta SNOTEL (snowpack telemetry) site <10 km to the north, and at a similar
211 elevation (Figure 1). Thus, it is likely that they represent rainstorms that delivered water less depleted in $\delta^{18}\text{O}$
212 relative to SMOW, a response reported in other studies (Krainer and Mostler, 2002). After these pulses are removed
213 from the data to highlight the background trends at each of the sites (Figure 6B), the record from the Spring is seen
214 to be the most stable, with nearly all values between -16 and -16.5‰. The water at RG-2, which started off similar
215 to the Spring, rises steadily to a maximum of -14‰ in early October. The Stream rises from -15.5‰ to -14‰ by the
216 third week of August, and stabilizes through the end of the record. Finally, RG-1, which also starts at -15.5‰, rises

217 rapidly in the first half of July, then more gradually until early September, when it peaks at -12.5% before dropping
218 to -13%.

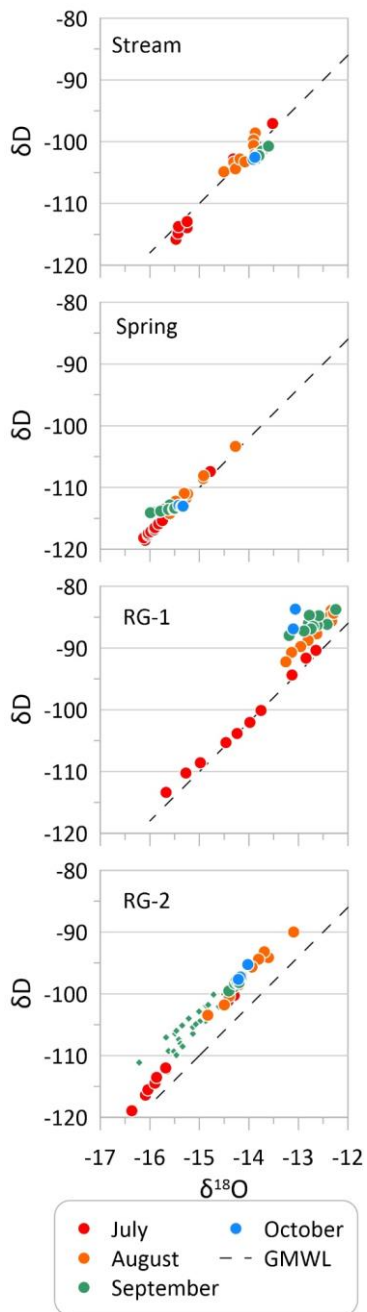
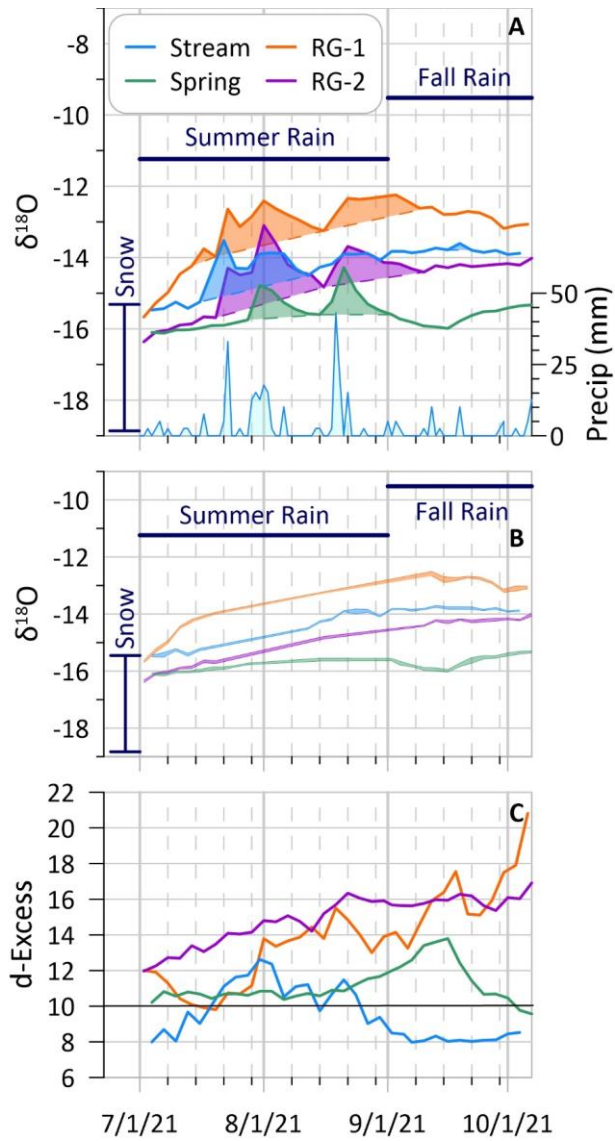


Figure 5: Dual isotope plots for the four individual time series. Color-coding represents the month of sample collection. The tendency for samples at the Stream and Spring to remain on the waterline while samples from the rock glaciers deviate to higher values of d -excess in late summer and fall is clearly evident. Green diamonds for RG-2 present reconnaissance data from September, 2020.



247

248 **Figure 6:** Time series from the four sampling sites. (A) Values of $\delta^{18}O$ presented along with average values for
 249 snow and rain, and daily precipitation recorded at the Chepeta SNOTEL site (Figure 1). (B) Same as Panel B with
 250 transient spikes in $\delta^{18}O$ due to precipitation events removed. Line width represents ± 1 standard deviation. (C)
 251 Times series of *d-excess*. The reference value of 10‰ is highlighted.

252 Values of *d-excess* in the time-series exhibit varying patterns (Figure 6C). Values from the Stream initially rise,
253 then fall through August and stabilize at 8‰ in the fall. The Spring samples are initially stable between 10 and
254 11‰, then rise in early September to a high of 14‰, before falling back to 10‰. The two rock glaciers sites, in
255 contrast, rise steadily from near 10‰, to ≥17‰ in early October (Figure 6C).

256 Context for the isotope values from the water samplers is provided by the precipitation samples collected at
257 the Spring and RG-2 sites, and grab samples of snow from RG-1 and RG-2 (Figure 6). Values of $\delta^{18}\text{O}$ in
258 composited July and August precipitation at the Spring and RG-2 sites average -11.2‰, and fall precipitation
259 averages -9.5‰. ~~snow~~ Values of $\delta^{18}\text{O}$ in snow samples are lower, averaging -17‰ (with *d-excess* ~10‰) with a
260 range from -15.3 to -18.6‰. This wide range is not surprising given that the stable isotopic composition of snow
261 can vary spatially across complex mountain terrain (Dietermann and Weiler, 2013), and can evolve through winter
262 sublimation and (Taylor et al., 2001; Earman et al., 2006; Lechler and Niemi, 2011) the process of snowpack melting
263 (Taylor et al., 2001; Unnikrishna et al., 2002; Earman et al., 2006; Lechler and Niemi, 2011) (e.g. Lechler and
264 Niemi, 2011). Nonetheless, these measurements are consistent with other reported snow samples from the Uintas
265 (Munroe, 2021) and with values predicated by the OIPC (Bowen and Wilkinson, 2002; Bowen and Revenaugh,
266 2003). Thus, in contrast, bulk precipitation falling in July and August at the Spring and RG-2 averages -11.2‰, and
267 fall precipitation averages -9.5‰. Values of *d-excess* in snow samples are ~10‰, whereas values in rain samples
268 are 13 to 21‰; they are considered to provide a reasonable constraint on the isotopic composition of snow within the
269 study area.

Formatted: Not Highlight

Formatted: Not Highlight

Formatted: Not Highlight

Formatted: Not Highlight

Formatted: Not Highlight

Field Code Changed

Field Code Changed

270 Hydrochemical analysis with ICP-MS reveals 12 elements that are consistently detectable in these samples:
271 Ba, Ca, Fe, K, Mg, Mn, Na, Ni, Rb, Si, Sr, and Ti. Ca and Si are generally the most abundant cations, with mean
272 abundance ~1500 to 2000 ppb, followed by K, Na and Mg with abundances averaging 500-800 ppb. Fe and Ba are
273 generally present at abundances around 100 ppb; other elements are present at lower concentrations (Table 3).
274 ~~Principle~~ Principal component analysis of these elemental concentrations, conducted with a varimax rotation, places
275 five elements (Ba, Ca, Na, Mg, Ni) on the first component (PC-1), with Ti, Rb, Si, K, Sr, and Mn on the second
276 (PC-2). Together these two components explain 78% of the variance. Highest values of PC-1 are found in the
277 Spring samples, followed by the Stream and the two rock glaciers. In contrast, PC-2 is highest at the rock glacier
278 sites and lower in the Stream and Spring. Plotting of PC-1 vs. PC-2 reveals a nearly complete separation between
279 the rock glacier water and samples from the Stream and Spring (Figure 7). When considered as time-series, values
280 of both components are generally stable at the Stream and Spring, but rise consistently through the summer and fall
281 at RG-1 and RG-2 (Figure 8).

282 The same 12 cations were generally detectable in the precipitation samples, with the exception of Fe, which
283 was typically below the detection limit. Values of Na, K, Mn, Rb, Fe, Ni, and Sr were higher in snow samples
284 relative to rain, with particularly high values of Na and K in the July snow sample from the RG-2 site (Figure 9). In
285 contrast, Ca, Ti, Ba, Mg, and Si were more abundant in rain samples. All elements were less abundant in rain than
286 in the time-series.

287

288 **5 Discussion**

289 **5.1 Isotopes and Hydrochemistry**

290 The automated samplers utilized in this project were successful at collecting essentially uninterrupted sequences of
 291 water throughout their deployment. Modification of the samplers effectively reduced evaporation-related
 292 fractionation that could have skewed the results over the long duration deployments. As seen in Figure 3, analysis
 293 of the subsample from the first sample bottle that was removed in early July yielded similar results to the water that
 294 remained inside the sampler until September. Values of δD and $\delta^{18}O$ overlap within error for RG-2 and are very

Table 3: Summary Hydrochemistry

	Na (ppb)	K (ppb)	Ca (ppb)	Ti (ppb)	Mn (ppb)	Rb (ppb)	Ba (ppb)	Mg (ppb)	Si (ppb)	Fe (ppb)	Ni (ppb)	Sr (ppb)
Stream (n=31)												
Mean	848.2	465.8	1636.9	3.2	3.9	0.4	64.6	496.0	1053.2	66.9	0.8	9.0
Median	790.0	347.3	1635.9	3.2	2.4	0.3	61.6	499.7	1056.7	49.3	0.6	9.0
Standard Deviation	199.6	393.4	77.9	0.3	4.7	0.1	8.9	17.2	79.9	80.0	0.4	0.9
Minimum	605.4	262.6	1471.5	2.5	0.7	0.2	56.2	451.5	866.0	0.0	0.2	7.7
Maximum	1325.4	2264.8	1836.5	4.2	23.2	0.9	92.3	528.9	1176.2	410.1	1.6	11.2
Spring (n=33)												
Mean	1075.5	499.9	1997.5	4.4	3.3	0.3	115.6	599.0	2034.7	34.7	0.7	11.0
Median	1104.8	513.1	1860.8	3.9	3.2	0.3	104.2	579.6	2048.8	20.1	0.5	10.8
Standard Deviation	284.8	107.3	313.0	0.9	1.6	0.1	34.9	56.8	84.4	33.6	0.6	1.1
Minimum	685.5	306.8	1764.4	3.6	1.1	0.2	90.7	517.4	1816.1	7.3	0.2	9.0
Maximum	2147.7	877.6	3100.8	7.5	6.7	0.7	251.1	770.6	2204.3	164.1	2.9	14.1
RG-1 (n=33)												
Mean	619.8	612.0	1587.5	12.5	12.3	1.2	53.6	527.9	2265.6	277.3	0.7	12.3
Median	633.4	602.9	1550.2	11.5	4.3	1.1	52.6	506.7	2145.7	234.1	0.7	11.7
Standard Deviation	123.5	207.3	396.4	6.3	30.8	0.7	18.8	132.0	1008.7	215.0	0.4	4.3
Minimum	380.9	259.0	938.2	3.5	1.4	0.2	27.7	309.0	678.5	18.1	0.1	5.6
Maximum	898.9	1081.6	2527.2	25.8	173.6	2.6	120.5	830.7	4108.3	1041.1	1.8	20.8
RG-2 (n=34)												
Mean	573.6	388.7	1289.7	6.1	8.1	0.7	43.3	396.9	1301.1	127.7	0.3	7.6
Median	570.9	372.2	1257.2	4.8	2.7	0.5	36.9	380.0	1225.0	56.3	0.2	7.0
Standard Deviation	170.6	95.0	257.4	4.1	14.2	0.4	17.3	87.3	444.9	174.2	0.3	2.7
Minimum	338.7	249.0	852.3	1.3	0.4	0.1	23.9	266.7	568.9	0.0	0.0	3.7
Maximum	883.8	592.8	1849.8	22.5	60.6	2.0	95.4	621.9	2323.0	764.2	1.8	15.1

295

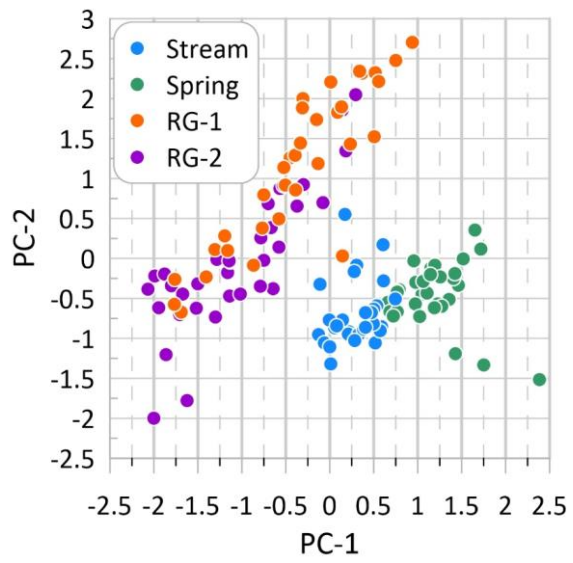
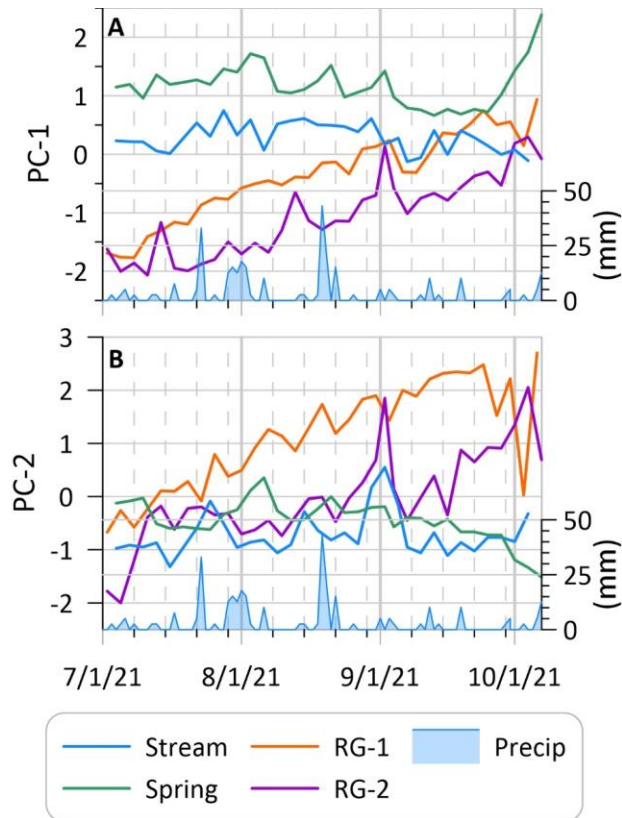


Figure 7: Biplot of the first and second ~~principle~~principal components determined for major elements in the water samples. The similarity of the rock glacier water samples is clear, as is their lack of overlap with the Stream and Spring samples.



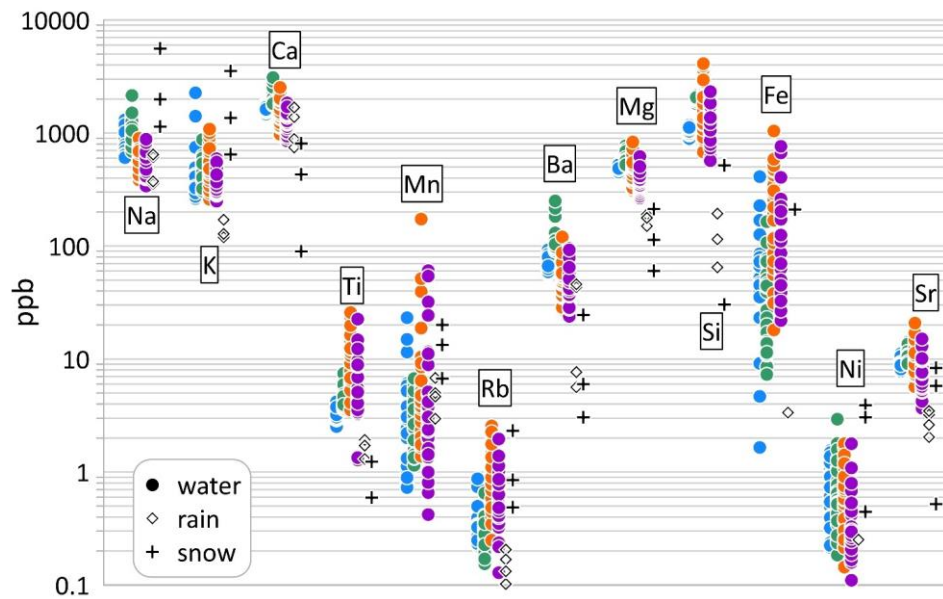
310

311 **Figure 8:** Time series of the first and second ~~principle~~ principal components presented in Figure 7. Values tend to be
 312 stable through the melt season at the Stream and Spring, but rise notably at both the rock glacier sites.

313

314 close for the Stream and Spring. There is a slight ~~tendency for increase in~~ $\delta^{18}\text{O}$ ~~to increase of~~ $\sim 0.2\%$ over the course
 315 of the summer, which ~~is consistent with~~ ~~could indicate~~ evaporation, however this shift is far less than the changes
 316 observed in these sequences of samples from start to finish. Thus, the time-series are interpreted without significant
 317 concern that values were altered by evaporation.

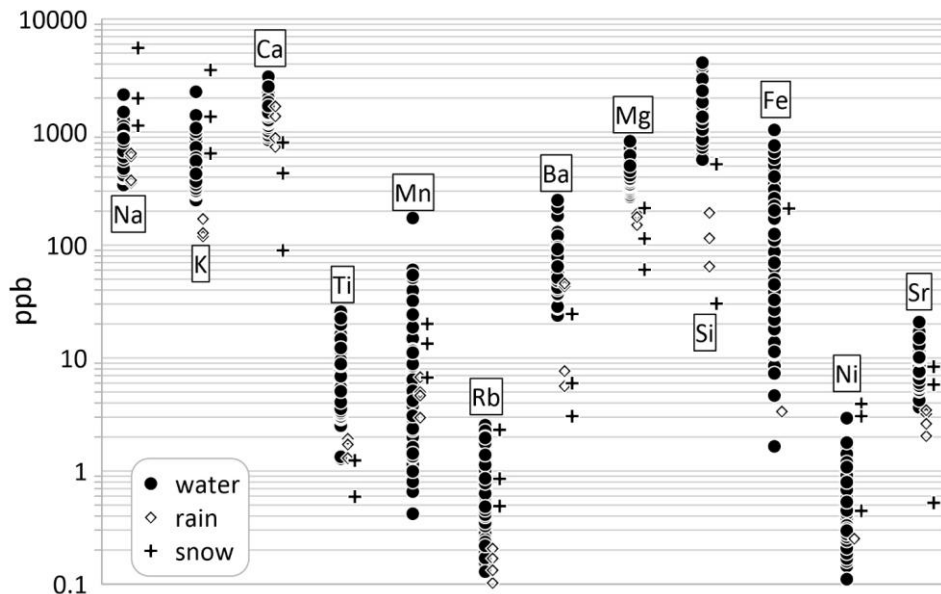
318 The sampling and analysis strategy in this project was designed to evaluate whether water draining from
 319 representative rock glaciers in the Uinta Mountains differs from ~~streamwaters~~ ~~streamwater~~ and ~~ground~~
 320 ~~water~~ ~~groundwater~~ in a manner that is consistent with the presence of melting ice within the rock glacier. The
 321 summer of 2021 was a particularly appropriate time to attempt this because the snowpack during the preceding
 322 winter was notably below average. On



323
 324 **Figure 9:** Abundances of detectable elements in the time series of water samples, along with the rain and snow
 325 samples. Water samples are presented from left to right with the same color designations as previous figures: Blue =
 326 stream, Green = Spring, Orange = RG-1, and Purple = RG-2. Note the logarithmic scale on the Y-axis.

327 April 1, 2021 the Chepeta SNOTEL (Figure 1) was at 83% of the 1991-2020 median of 380 mm snow water

Formatted: Indent: First line: 0"



328
329 **Figure 9.** Abundances of detectable elements in the time series of water samples, along with the rain and snow
330 samples. Note the logarithmic scale on the Y axis.

331 equivalent (SWE), but by April 13, the average date of the annual peak, SWE was just 52% of average (188 mm).
332 In contrast to other years in which we have conducted fieldwork at the RG-1 and RG-2 sites, the surfaces of the rock
333 glaciers were notably snow free when the samplers were deployed in early July. Inspection of high-resolution
334 satellite imagery confirms that visible snow on the rock glacier surfaces disappeared by the end of June, and that
335 essentially no snow was present anywhere in the West Fork Whiterocks Drainage after the start of July. Therefore,
336 it is unlikely that the water collected at RG-1 and RG-2, particularly late summer and fall, was sourced from melting
337 snow.

338 Analysis of stable isotopes reveals contrast between the water types that can be linked back to their sources
339 and flowpaths. Groundwater from the spring exhibits the most depleted $\delta^{18}\text{O}$, with values similar to the snow
340 samples (Figure 6). This. The snow samples span a relatively wide range of $\delta^{18}\text{O}$, but they are the most negative
341 measured in this study, thus this correspondence suggests that the groundwater system is primarily recharged by
342 snowmelt. The average annual maximum SWE at the Chepeta SNOTEL station of 380 mm equals half of the mean
343 annual precipitation. The snowmelt pulse in the spring, therefore, is apparently the only precipitation event of the
344 year that can overwhelm the moisture holding capacity of the soil and pass water into the groundwater system. The
345 consistently low $\delta^{18}\text{O}$ values of the water discharging from the spring during the course of the summer, despite

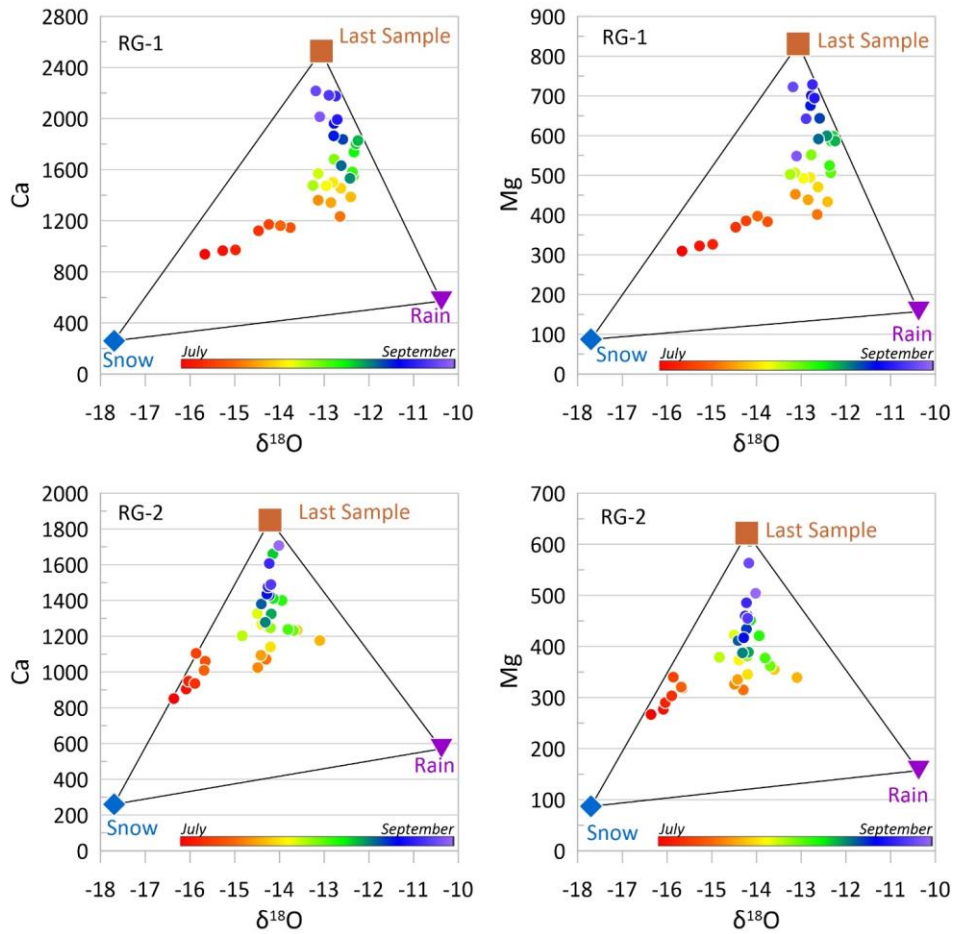
346 numerous rainstorms delivering isotopically less depleted water, emphasizes that the deeper groundwater system is
347 snow-dominated and stable.

348 Samples from RG-1 and RG-2 from ~~the early part of the melt season plot~~ July plot on the GMWL, with low
349 values of δD and $\delta^{18}O$ consistent with a large ~~contribution component~~ of snowmelt (Figure 5), which is isotopically
350 ~~depleted in this study and in values reported from elsewhere in the Uintas~~ (Munroe, 2021) ~~(Figure 5)~~. Even though
351 visible snow was absent from the rock glacier surfaces at this time, this correspondence indicates that snow was still
352 melting within the interstices between blocks on the rock glacier surface, a situation that was reported by previous
353 ~~studies work~~ (Krainer et al., 2007). By the beginning of August, however, isotope values at both rock glacier
354 springs depart from the GMWL and rise to higher values of *d-excess* (Figure 5). This pattern is not seen in the
355 Spring or the Stream time-series, which remain on the GMWL from start to finish. Thus, late summer and fall water
356 discharging from both rock glaciers is distinct from contemporary precipitation and ~~ground water~~ groundwater. This
357 pattern is particularly dramatic at RG-1, where all of the August through October samples cluster around a $\delta^{18}O$ of -
358 13‰ with *d-excess* values as high as 20‰. Previous work on rock glacier hydrology has reported high values of *d-*
359 *excess* in late-summer rock glacier discharge, and interpreted them as a signal of melting internal rock glacier ice
360 that has undergone numerous freeze/thaw cycles (Steig et al., 1998; Williams et al., 2006).

361 The time-series of PC values reinforce the uniqueness of the rock glacier water. Values for the Spring and
362 for the Stream are notably stable through the ~~melt season~~ summer and into the fall (Figure 8). This consistency
363 suggests that these systems are not directly impacted by short-term events like rainstorms, or even changes over
364 seasonal timescales, presumably due to their well-mixed nature and large ~~reservoirs~~ volumes. In contrast, the time
365 series for the two rock glacier springs ~~exhibit a dramatic rise~~ rise dramatically during the melt season. Values of PC-
366 1 increase starting at the beginning of July in both records; values of PC-2 start rising in July for RG-1 and in mid-
367 August for RG-2. Concentrations for many ~~individual~~ elements increase by a factor of 3 or more from early July
368 until October. This enrichment is consistent with movement of water through the fine matrix of crushed rock
369 material in the rock glacier interior, where fresh mineral grains are available for rapid chemical weathering by cold
370 water charged with carbonic acid (Krainer and Mostler, 2002; Williams et al., 2006). Melting of ice would both
371 liberate meltwater and open flowpaths through this material. The pattern of rising dissolved load through the
372 summer, therefore, provides additional support for the interpretation that the source of the water draining from the
373 rock glaciers shifts after snowmelt is over.

374 The transition in source of the water draining from the rock glaciers is further illustrated by biplots of $\delta^{18}O$
375 against Ca and Mg content (Figure 10). Values for ~~average~~ snow, rain, and the last sample from each rock glacier
376 define a triangle entirely enclosing samples collected from the rock glaciers. Water draining from the rock glaciers
377 in July exhibits a clear snowmelt influence, but this diminishes in August as the water becomes a more even mixture
378 of rain and rock glacier water. Through September into October, this balance shifts away from rain, eventually
379 reaching a minimal rain contribution in the last water discharged before the system froze up for the winter. ~~Even~~
380 ~~considering the inherent uncertainty imparted by the small number of precipitation samples, it is obvious that the~~
381 ~~rock glacier water composition evolves away from snow and rain over the course of the melt season~~ (Figure 10).

382 Williams et al. (2006) proposed a model for changing flowpaths and water sources over the course of the
 383 melt season that is relevant for interpreting the results presented here. In early summer, the interior of a rock glacier
 384 is frozen and water derived from snowmelt is discharged after draining through the blocky surface layer and running
 385 along the top of the frozen core (Krainer and Mostler, 2002). Later in the summer, snowmelt is finished and
 386 seasonal ice within the rock glacier begins to melt, opening flowpaths that bring meltwater into contact with fresh

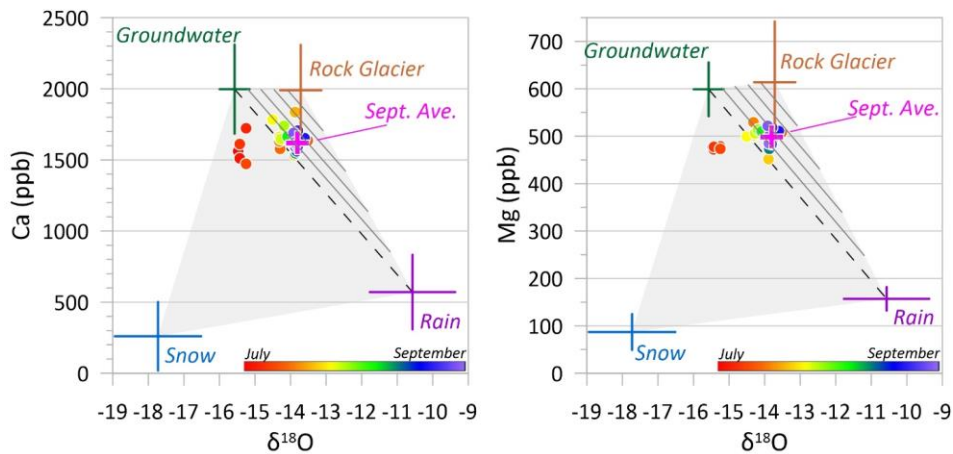


387
 388 **Figure 10:** Biplots of $\delta^{18}O$ vs. Ca and Mg at RG-1 and RG-2. Circles represent water discharging from the rock
 389 glacier springs, with the rainbow pattern progressing from early July (red) through to early October (purple). The
 390 last sample collected at each rock glacier is plotted as the brown square, along with average values for snow and
 391 rain. Rock glacier water clearly evolves through the season from a composition dominated by snowmelt, to a
 392 mixture of rain and internal water, with decreasing rain influence over time.

393 highly weatherable mineral grains. Finally, in late summer and the fall, older perennial ice within the rock glacier
 394 begins to melt (Williams et al., 2007), liberating water with high dissolved load and uniquely high values of *d-excess*
 395 due reflecting a history of multiple freeze/thaw cycles. The isotopic and hydrochemical results presented here are
 396 consistent with this model, supporting the interpretation that water discharging from Uinta rock glaciers in late
 397 summer and fall is derived from the melting of perennial internal ice.

398 5.2 Implications for High Mountain Hydrology

399 The rock glaciers studied in this project are but two of eight mapped (Figure 1) within the West Fork Whiterocks
 400 watershed (Munroe, 2018), which also hosts extensive talus (Munroe and Laabs, 2009) that may contain non-trivial
 401 amounts of ice. It is reasonable to predict, therefore, that water derived from rock glaciers may comprise an
 402 important amount of the overall streamflow in the latter part of the summer and fall. Figure 11 presents biplots of
 403 $\delta^{18}\text{O}$ vs. Ca and Mg content, two elements that are notably elevated in the late summer rock glacier water in the
 404 Uintas and elsewhere (Williams et al., 2006).



405
 406 **Figure 11:** Biplots of $\delta^{18}\text{O}$ vs. Ca and Mg used to determine the contribution of rock glacier discharge to
 407 streamflow. Water in the stream is plotted with a rainbow pattern progressing from July (red) through to early
 408 October (purple). Crosses represent the end members of snow, rain, groundwater, and rock glacier water. July
 409 ~~streamwater~~ streamwater samples contain a mixture of snowmelt and groundwater, but in August and September,
 410 snowmelt is now longer detectable (samples to right of dashed line). ~~Streamwater~~ Streamwater samples at this time
 411 contain non-trivial amounts of water derived from rock glaciers, with an average of 25% in September (pink cross).
 412 Diagonal black lines denote the abundance of rock glacier water in increments of 20% for emphasis.

413 After Krainer and Mostler (2002), four end member sources of water to the stream are: groundwater, snow, rain, and
 414 rock glaciers. The groundwater end member is constrained for the 2021 melt season by the 33 samples from the

415 non-rock glacier spring. ~~The As noted above, the~~ snow end member is less well constrained, however ~~the two grab~~
416 ~~samples collected in July from RG-1 and RG-2 have isotope values consistent with snow previously analyzed from~~
417 ~~the Uintas (Munroe, 2021) and with values predicted by the OPIC. Thus~~ these samples are ~~nonetheless~~ considered a
418 valid representation of the snow lingering in the Whiterocks River watershed in the summer of 2021. Five samples
419 (two from RG-1 and three from RG-2) collected from the rock glacier springs in October immediately before freeze
420 up represent the rock glacier meltwater end member. Finally, two ~~composite~~ precipitation samples from RG-2 and
421 two from the spring site are available to represent rain ~~falling over the course of the melt season. However~~ ~~Close~~
422 ~~inspection reveals, however, that~~; the concentration of Ca in the Spring sampler is ~3x higher than at RG-2, despite
423 the distance of only 3 km between the two sites. The precipitation sampler at the Spring site is located close to a dirt
424 road though, raising the possibility that dust produced by vehicle traffic raised the Ca content of the water collected
425 at this site. Support for this interpretation is provided by 7 years of unpublished precipitation chemistry (n=79
426 samples) collected by the USDA-Ashley National Forest in the Uintas. Concentrations of Ca in this dataset average
427 645 ppb, similar to the value of 570 ppb in the rain from the precipitation sampler at RG-2 and notably less than
428 mean of 1535 ppb at the roadside Spring site. Thus, the precipitation samples from RG-2 alone are taken to
429 represent the rain end member in the stream system for the melt season of 2021.

430 With this approach, the four end members define a polygon entirely surrounding the
431 ~~streamwater~~ ~~streamwater~~ samples (Figure 11). As in the time-series from the individual rock glaciers (Figure 5), a
432 clear transition is notable. July ~~streamwater~~ ~~streamwater~~ samples exhibit $\delta^{18}\text{O}$ values similar to snowmelt and
433 groundwater. ~~In contrast, whereas~~ late summer and fall samples plot ~~far from the snowmelt end member and~~
434 entirely within a triangle bounded by the groundwater, rock glacier ~~water~~, and rain. Within this triangle, although
435 the proportions vary somewhat between samples, individual ~~streamwater~~ ~~streamwater~~ samples from August and
436 September can be visually separated as a mixture of ~20-30% rain, ~25 to 75% groundwater, and up to 50% rock
437 glacier water. The overall mean of September ~~streamwater~~ ~~streamwater~~ samples can be defined as ~25% rain, ~50%
438 groundwater, and ~25% rock glacier water. Water with a signature similar to that of springs discharging directly
439 from rock glacier termini, therefore, generally makes up ~~approximately one~~ a quarter of all the water flowing in the
440 master stream of this drainage after snowmelt has ended.

441 ~~With~~ ~~Given the detectable~~ ~~such a significant~~ contribution of rock glacier meltwater to streamflow in this
442 system, it is worth considering whether rock glacier ice is melting at an unsustainable rate. This possibility is hard
443 to evaluate directly, given that mass balance techniques for ice glacier systems are difficult to apply to rock glaciers
444 (Østrem and Brugman, 1966). Nonetheless, it is notable that a depression consistent with subsidence accompanying
445 the melt-out of an ice core is present in the upper part of RG-2 (Figure 12). A high-resolution topographic model
446 constructed for this rock glacier using structure-from-motion applied to images collected with an uncrewed aerial
447 vehicle (UAV) reveals that this depression has an area of 19,350 m² and a volume of 106,500 m³ (mean depth of 5.5
448 m). If this depression formed due to the loss of ice, this volume corresponds to ~10⁸ L of water. At rates of 10² to
449 10³ L/min estimated for the modern flow, that equates to 70 to 700 days. ~~This calculation is inherently general~~
450 ~~given the uncertainty around the age and timing of the depression, and the true rates of water discharge.~~

451 Nonetheless, the presence of this depression and its dimensions suggests that ~~Thus,~~ ice within this rock glacier may
452 have begun melting unsustainably in the past few decades in response to rising summer temperatures noted in Uinta
453 climate records (Brencher et al., 2021). Future InSAR monitoring may help constrain subsidence on this and other
454 rock glaciers, yielding additional information about the response of these features to contemporary climate warming
455 and likely changes in their future contributions to high-elevation hydrology.

456

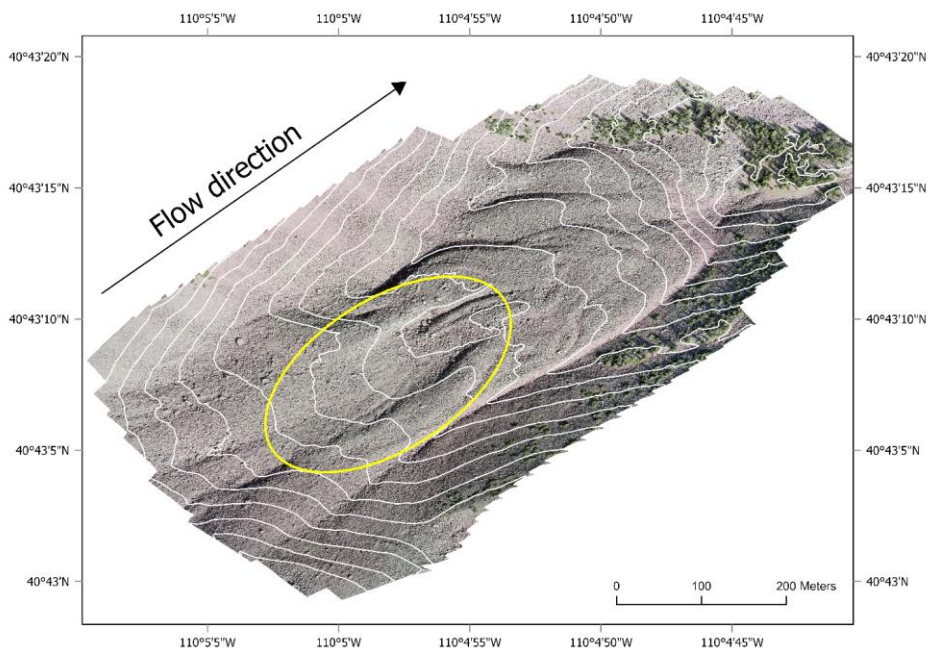
457

458 **6 Conclusion**

459 Time series of samples collected during the summer of 2021 reveal that water draining from rock glaciers in the
460 Uinta Mountains of Utah (USA) has a composition distinct from groundwater and from water in the master stream



461



462
 463 **Figure 12:** True-color hillshaded photomosaic of RG-2 produced by structure from motion (SfM) applied to a set of
 464 243 images collected at an altitude of 120 m above the ground. White lines represent 10-m contours and the black
 465 arrow designates the downslope flow direction. The white-yellow oval highlights the prominent depression near the
 466 head of the rock glacier, which may reflect subsidence due to ice meltout.

467
 468 of a representative 5000-ha drainage. Rock glacier water resembles snowmelt in the early summer, but transitions to
 469 higher values of *d-excess* and greatly elevated Ca and Mg content as the melt season progresses. This pattern is
 470 consistent with models describing a change in water source from snowmelt, to melting of seasonal ice, to melting of
 471 deeper perennial ice in the rock glacier interior in late summer and fall. Water derived from this internal ice appears
 472 to have been the source of ~25% of the streamflow in this study area during September of 2021. This result
 473 emphasizes the significant role that rock glaciers can play in the hydrology of high-elevation watersheds,
 474 particularly in melt seasons following a winter with below average snowpack.

475
 476 **Data Availability**

477 [The stable isotope and hydrochemical data generated in this study are available in the Hydroshare data repository at](http://www.hydroshare.org/resource/2db20d7810254489b14984ef282951e1)
478 <http://www.hydroshare.org/resource/2db20d7810254489b14984ef282951e1>.

Formatted: Font: Not Bold

479

480 **Author Contributions**

481 JM designed the project, conducted the fieldwork and laboratory analyses, interpreted the results, and drafted the
482 figures. JS prepared the manuscript with contributions from AH.

483

484 **Competing Interests:** The authors declare that they have no conflict of interest.

485

486 **Acknowledgements**

487 This work was supported by NSF HS-1935200 to PIs Munroe and Handwerger, and NSF MRI-1918436 to Munroe.
488 The authors thank Q. Brencher, C. Kluetmeier, S. Lusk, E. Norris, A. Santis, and A. Takoudes for their assistance in
489 the field, and E. McMahon for help preparing the water samplers.

490 **References Cited**

- 491 Adler, C., Huggel, C., Orlove, B., and Nolin, A., 2019, Climate change in the mountain cryosphere: impacts and
492 responses: *Regional Environmental Change*, v. 19, p. 1225–1228.
- 493 Albrich, K., Rammer, W., and Seidl, R., 2020, Climate change causes critical transitions and irreversible alterations
494 of mountain forests: *Global change biology*, v. 26, p. 4013–4027.
- 495 Alexander, J.M., Chalmandrier, L., Lenoir, J., Burgess, T.I., Essi, F., Haider, S., Kueffer, C., McDougall, K.,
496 Milbau, A., and Nuñez, M.A., 2018, Lags in the response of mountain plant communities to climate
497 change: *Global change biology*, v. 24, p. 563–579.
- 498 Atwood, W.W., 1909, *Glaciation of the Uinta and Wasatch mountains*: US Government Printing Office, v. 61.
- 499 Azócar, G.F., and Brenning, A., 2010, Hydrological and geomorphological significance of rock glaciers in the dry
500 Andes, Chile (27–33 S): *Permafrost and Periglacial Processes*, v. 21, p. 42–53.
- 501 Beniston, M., Farinotti, D., Stoffel, M., Andreassen, L.M., Coppola, E., Eckert, N., Fantini, A., Giacona, F., Hauck,
502 C., and Huss, M., 2018, The European mountain cryosphere: a review of its current state, trends, and future
503 challenges: *The Cryosphere*, v. 12, p. 759–794.
- 504 Biskaborn, B.K. et al., 2019, Permafrost is warming at a global scale: *Nature Communications*, v. 10, p. 264,
505 doi:10.1038/s41467-018-08240-4.
- 506 Bonfils, C., Santer, B.D., Pierce, D.W., Hidalgo, H.G., Bala, G., Das, T., Barnett, T.P., Cayan, D.R., Doutriaux, C.,
507 and Wood, A.W., 2008, Detection and attribution of temperature changes in the mountainous western
508 United States: *Journal of Climate*, v. 21, p. 6404–6424.
- 509 Bowen, G.J., and Revenaugh, J., 2003, Interpolating the isotopic composition of modern meteoric precipitation:
510 *Water Resources Research*, v. 39, <http://onlinelibrary.wiley.com/doi/10.1029/2003WR002086/full>
511 (accessed January 2017).
- 512 Bowen, G.J., and Wilkinson, B., 2002, Spatial distribution of $\delta^{18}\text{O}$ in meteoric precipitation: *Geology*, v. 30, p.
513 315–318.
- 514 Brencher, G., Handwerger, A.L., and Munroe, J.S., 2021, InSAR-based characterization of rock glacier movement
515 in the Uinta Mountains, Utah, USA: *The Cryosphere*, v. 15, p. 4823–4844.
- 516 Brighenti, S., Hotaling, S., Finn, D.S., Fountain, A.G., Hayashi, M., Herbst, D., Saros, J.E., Tronstad, L.M., and
517 Millar, C.I., 2021, Rock glaciers and related cold rocky landforms: Overlooked climate refugia for
518 mountain biodiversity: *Global Change Biology*, v. 27, p. 1504–1517.
- 519 Buchli, T., Kos, A., Limpach, P., Merz, K., Zhou, X., and Springman, S.M., 2018, Kinematic investigations on the
520 Furggwanhom rock glacier, Switzerland: *Permafrost and Periglacial Processes*, v. 29, p. 3–20.
- 521 Catalan, J., Ninot, J.M., and Aniz, M.M., 2017, *High mountain conservation in a changing world*: Springer Nature.
- 522 Chakraborty, A., 2021, Mountains as vulnerable places: a global synthesis of changing mountain systems in the
523 Anthropocene: *GeoJournal*, v. 86, p. 585–604.
- 524 Craig, H., 1961, Isotopic variations in meteoric waters: *Science*, v. 133, p. 1702–1703.
- 525 Dansgaard, W., 1964, Stable isotopes in precipitation: *Tellus*, v. 16, p. 436–468.

Formatted: Font: (Default) Times New Roman

- 526 Dehler, C.M., Porter, S.M., De Grey, L.D., Sprinkel, D.A., and Brehm, A., 2007, The Neoproterozoic Uinta
527 Mountain Group revisited; a synthesis of recent work on the Red Pine Shale and related undivided clastic
528 strata, northeastern Utah, U. S. A (P. K. Link & R. S. Lewis, Eds.): Special Publication - Society for
529 Sedimentary Geology, v. 86, p. 151–166.
- 530 Dietermann, N., and Weiler, M., 2013, Spatial distribution of stable water isotopes in alpine snowcover: Hydrology
531 and Earth System Sciences, v. 17, p. 2657–2668.
- 532 Earman, S., Campbell, A.R., Phillips, F.M., and Newman, B.D., 2006, Isotopic exchange between snow and
533 atmospheric water vapor: Estimation of the snowmelt component of groundwater recharge in the
534 southwestern United States: Journal of Geophysical Research: Atmospheres, v. 111.
- 535 Egan, P.A., and Price, M.F., 2017, Mountain ecosystem services and climate change: A global overview of potential
536 threats and strategies for adaptation:
- 537 von Freyberg, J., Knapp, J.L.A., Rücker, A., Studer, B., and Kirchner, J.W., 2020, Technical note: Evaluation of a
538 low-cost evaporation protection method for portable water samplers: Hydrology and Earth System
539 Sciences, v. 24, p. 5821–5834, doi:10.5194/hess-24-5821-2020.
- 540 Geiger, S.T., Daniels, J.M., Miller, S.N., and Nicholas, J.W., 2014, Influence of rock glaciers on stream hydrology
541 in the La Sal Mountains, Utah: Arctic, Antarctic, and Alpine Research, v. 46, p. 645–658.
- 542 Giardino, J.R., Shroder, J.F., and Vitek, J.D., 1987, Rock glaciers: Allen & Unwin London.
- 543 Giardino, J.R., and Vitek, J.D., 1988, The significance of rock glaciers in the glacial-periglacial landscape
544 continuum: Journal of Quaternary Science, v. 3, p. 97–103, doi:10.1002/jqs.3390030111.
- 545 Gröning, M., Lutz, H.O., Roller-Lutz, Z., Kralik, M., Gourcy, L., and Pölsenstein, L., 2012, A simple rain collector
546 preventing water re-evaporation dedicated for $\delta^{18}\text{O}$ and $\delta^2\text{H}$ analysis of cumulative precipitation samples:
547 Journal of Hydrology, v. 448, p. 195–200.
- 548 Halla, C., Blöthe, J.H., Tapia Baldis, C., Trombotto Liaudat, D., Hilbich, C., Hauck, C., and Schrott, L., 2021, Ice
549 content and interannual water storage changes of an active rock glacier in the dry Andes of Argentina: The
550 Cryosphere, v. 15, p. 1187–1213.
- 551 Hansen, W.R., 1986, Neogene tectonics and geomorphology of the eastern Uinta Mountains in Utah, Colorado, and
552 Wyoming: United States Geological Survey, Professional Paper, v. 75.
- 553 Harrington, J.S., Mozil, A., Hayashi, M., and Bentley, L.R., 2018, Groundwater flow and storage processes in an
554 inactive rock glacier: Hydrological Processes, v. 32, p. 3070–3088.
- 555 Huss, M., Bookhagen, B., Huggel, C., Jacobsen, D., Bradley, R.S., Clague, J.J., Vuille, M., Buytaert, W., Cayan,
556 D.R., and Greenwood, G., 2017, Toward mountains without permanent snow and ice: Earth's Future, v. 5,
557 p. 418–435.
- 558 Janke, J.R., Ng, S., and Bellisario, A., 2017, An inventory and estimate of water stored in firn fields, glaciers,
559 debris-covered glaciers, and rock glaciers in the Aconcagua River Basin, Chile: Geomorphology, v. 296, p.
560 142–152.
- 561 Johnson, G., Chang, H., and Fountain, A., 2021, Active rock glaciers of the contiguous United States: geographic
562 information system inventory and spatial distribution patterns: Earth System Science Data, v. 13, p. 3979–
563 3994, doi:10.5194/essd-13-3979-2021.

- 564 Jones, D.B., Harrison, S., Anderson, K., Selley, H.L., Wood, J.L., and Betts, R.A., 2018, The distribution and
565 hydrological significance of rock glaciers in the Nepalese Himalaya: *Global and Planetary Change*, v. 160,
566 p. 123–142.
- 567 Jones, D.B., Harrison, S., Anderson, K., and Whalley, W.B., 2019, Rock glaciers and mountain hydrology: A
568 review: *Earth-Science Reviews*, v. 193, p. 66–90, doi:10.1016/j.earscirev.2019.04.001.
- 569 Kenner, R., Phillips, M., Limpach, P., Beutel, J., and Hiller, M., 2018, Monitoring mass movements using
570 georeferenced time-lapse photography: Ritigraben rock glacier, western Swiss Alps: *Cold Regions Science
571 and Technology*, v. 145, p. 127–134.
- 572 Konrad, S.K., Humphrey, N.F., Steig, E.J., Clark, D.H., Potter, N., and Pfeffer, W.T., 1999, Rock glacier dynamics
573 and paleoclimatic implications: *Geology*, v. 27, p. 1131–1134.
- 574 Krainer, K. et al., 2015, A 10,300-year-old permafrost core from the active rock glacier Lazaun, southern Ötztal
575 Alps (South Tyrol, northern Italy): *Quaternary Research*, v. 83, p. 324–335,
576 doi:10.1016/j.yqres.2014.12.005.
- 577 Krainer, K., and Mostler, W., 2002, Hydrology of active rock glaciers: examples from the Austrian Alps: *Arctic,
578 Antarctic, and Alpine Research*, p. 142–149.
- 579 Krainer, K., Mostler, W., and Spötl, C., 2007, DISCHARGE FROM ACTIVE ROCK GLACIERS, AUSTRIAN
580 ALPS: A STABLE ISOTOPE APPROACH.: *Austrian Journal of Earth Sciences*, v. 100.
- 581 Lechler, A.R., and Niemi, N.A., 2011, The influence of snow sublimation on the isotopic composition of spring and
582 surface waters in the southwestern United States: Implications for stable isotope-based paleoaltimetry and
583 hydrologic studies: *Geological Society of America Bulletin*, p. B30467-1.
- 584 Lehmann, B., Anderson, R.S., Bodin, X., Cusicanqui, D., Valla, P.G., and Carcaillet, J., 2022, Alpine rock glacier
585 activity over Holocene to modern timescales (western French Alps): *Earth Surface Dynamics Discussions*,
586 p. 1–40.
- 587 McDowell, G., Huggel, C., Frey, H., Wang, F.M., Cramer, K., and Ricciardi, V., 2019, Adaptation action and
588 research in glaciated mountain systems: Are they enough to meet the challenge of climate change? *Global
589 Environmental Change*, v. 54, p. 19–30.
- 590 Millar, C.I., and Westfall, R.D., 2010, Distribution and climatic relationships of the American pika (*Ochotona
591 princeps*) in the Sierra Nevada and western Great Basin, USA; periglacial landforms as refugia in warming
592 climates: *Arctic, Antarctic, and Alpine Research*, v. 42, p. 76–88.
- 593 Millar, C.I., Westfall, R.D., Evenden, A., Holmquist, J.G., Schmidt-Gengenbach, J., Franklin, R.S., Nachlinger, J.,
594 and Delany, D.L., 2015, Potential climatic refugia in semi-arid, temperate mountains: Plant and arthropod
595 assemblages associated with rock glaciers, talus slopes, and their forefield wetlands, Sierra Nevada,
596 California, USA: *Quaternary International*, v. 387, p. 106–121, doi:10.1016/j.quaint.2013.11.003.
- 597 Minder, J.R., Letcher, T.W., and Liu, C., 2018, The character and causes of elevation-dependent warming in high-
598 resolution simulations of Rocky Mountain climate change: *Journal of Climate*, v. 31, p. 2093–2113.
- 599 Munroe, J.S., 2018, Distribution, evidence for internal ice, and possible hydrologic significance of rock glaciers in
600 the Uinta Mountains, Utah, USA: *Quaternary Research*, v. 90, p. 1–16.
- 601 Munroe, J.S., 2021, First Investigation of Perennial Ice in Winter Wonderland Cave, Uinta Mountains, Utah, USA:
602 *The Cryosphere*, v. 15, p. 863–881, doi:doi.org/10.5194/tc-15-863-2021.

- 603 Munroe, J.S., 2006, Investigating the spatial distribution of summit flats in the Uinta Mountains of northeastern
604 Utah, USA: *Geomorphology*, v. 75, p. 437–449.
- 605 Munroe, J.S., and Laabs, B.J.C., 2009, *Glacial Geologic Map of the Uinta Mountains Area, Utah and Wyoming*.
606 Utah Geological Survey Miscellaneous Publication 09-4DM, scale Map.
- 607 Østrem, G., and Brugman, M., 1966, *Glacier mass balance measurements: Department of Mines and Technical
608 Surveys, Glaciology Section.*
- 609 Palomo, I., 2017, Climate change impacts on ecosystem services in high mountain areas: a literature review:
610 *Mountain Research and Development*, v. 37, p. 179–187.
- 611 Petersen, E.I., Levy, J.S., Holt, J.W., and Stuurman, C.M., 2020, New insights into ice accumulation at Galena
612 Creek Rock Glacier from radar imaging of its internal structure: *Journal of Glaciology*, v. 66, p. 1–10.
- 613 Rangecroft, S., Harrison, S., and Anderson, K., 2015, Rock Glaciers as Water Stores in the Bolivian Andes: An
614 Assessment of Their Hydrological Importance: *Arctic, Antarctic, and Alpine Research*, v. 47, p. 89–98,
615 doi:10.1657/AAAR0014-029.
- 616 Rödder, D., Schmitt, T., Gros, P., Ulrich, W., and Habel, J.C., 2021, Climate change drives mountain butterflies
617 towards the summits: *Scientific reports*, v. 11, p. 1–12.
- 618 Rowan, A.V., Quincey, D.J., Gibson, M.J., Glasser, N.F., Westoby, M.J., Irvine-Fynn, T.D., Porter, P.R., and
619 Hambrey, M.J., 2018, The sustainability of water resources in High Mountain Asia in the context of recent
620 and future glacier change: *Geological Society, London, Special Publications*, v. 462, p. 189–204.
- 621 Sakai, A., and Fujita, K., 2017, Contrasting glacier responses to recent climate change in high-mountain Asia:
622 *Scientific reports*, v. 7, p. 1–8.
- 623 Sears, J., Graff, P., and Holden, G., 1982, Tectonic evolution of lower Proterozoic rocks, Uinta Mountains, Utah and
624 Colorado: *Geological Society of America Bulletin*, v. 93, p. 990–997.
- 625 Sommer, C., Malz, P., Seehaus, T.C., Lippl, S., Zemp, M., and Braun, M.H., 2020, Rapid glacier retreat and
626 downwasting throughout the European Alps in the early 21st century: *Nature Communications*, v. 11, p. 1–
627 10.
- 628 Steig, E.J., Fitzpatrick, J.J., Potter, N., and Clark, D.H., 1998, The geochemical record in rock glaciers: *Geografiska
629 Annaler: Series A, Physical Geography*, v. 80, p. 277–286.
- 630 Stoffel, M., and Corona, C., 2018, Future winters glimpsed in the Alps: *Nature Geoscience*, v. 11, p. 458–460.
- 631 Strozzi, T., Caduff, R., Jones, N., Barboux, C., Delaloye, R., Bodin, X., Käab, A., Mätzler, E., and Schrott, L., 2020,
632 Monitoring rock glacier kinematics with satellite synthetic aperture radar: *Remote Sensing*, v. 12, p. 559.
- 633 Taylor, S., Feng, X., Kirchner, J.W., Osterhuber, R., Klaue, B., and Renshaw, C.E., 2001, Isotopic evolution of a
634 seasonal snowpack and its melt: *Water Resources Research*, v. 37, p. 759–769.
- 635 Thaler, T., Zischg, A., Keiler, M., and Fuchs, S., 2018, Allocation of risk and benefits—distributional justices in
636 mountain hazard management: *Regional environmental change*, v. 18, p. 353–365.
- 637 Unnikrishna, P.V., McDonnell, J.J., and Kendall, C., 2002, Isotope variations in a Sierra Nevada snowpack and their
638 relation to meltwater: *Journal of Hydrology*, v. 260, p. 38–57.
- 639 Wagner, T., Brodacz, A., Krainer, K., and Winkler, G., 2020, Active rock glaciers as shallow groundwater
640 reservoirs, Austrian Alps: *Grundwasser*, v. 25, p. 215–230.

- 641 Wagner, T., Kainz, S., Helfricht, K., Fischer, A., Avian, M., Krainer, K., and Winkler, G., 2021, Assessment of
642 liquid and solid water storage in rock glaciers versus glacier ice in the Austrian Alps: *Science of the Total*
643 *Environment*, v. 800, p. 149593.
- 644 Wahrhaftig, C., and Cox, A., 1959, Rock glaciers in the Alaska Range: *Geological Society of America Bulletin*, v.
645 70, p. 383–436.
- 646 Williams, M.W., Knauf, M., Caine, N., Liu, F., and Verplanck, P.L., 2006, Geochemistry and source waters of rock
647 glacier outflow, Colorado Front Range: *Permafrost and Periglacial Processes*, v. 17, p. 13–33,
648 doi:10.1002/ppp.535.
- 649 Williams, M.W., Knauf, M., Cory, R., Caine, N., and Liu, F., 2007, Nitrate content and potential microbial signature
650 of rock glacier outflow, Colorado Front Range: *Earth Surface Processes and Landforms*, v. 32, p. 1032–
651 1047, doi:10.1002/esp.1455.
- 652 Xenarios, S., Gafurov, A., Schmidt-Vogt, D., Sehring, J., Manandhar, S., Hergarten, C., Shigaeva, J., and Foggin,
653 M., 2019, Climate change and adaptation of mountain societies in Central Asia: uncertainties, knowledge
654 gaps, and data constraints: *Regional Environmental Change*, v. 19, p. 1339–1352.
- 655